Optics Letters

Optimal generation of high harmonics in the water-window region by synthesizing 800-nm and mid-infrared laser pulses

CHENG JIN,[1,2,*] KYUNG-HAN HONG,[3] AND C. D. LIN[1]

[1]J. R. Macdonald Laboratory, Department of Physics, Kansas State University, Manhattan, Kansas 66506, USA
[2]School of Science, Nanjing University of Science and Technology, Nanjing, Jiangsu 210094, China
[3]Department of Electrical Engineering and Computer Science and Research Laboratory of Electronics, Massachusetts Institute of Technology (MIT), Cambridge, Massachusetts 02139, USA
*Corresponding author: cjin@phys.ksu.edu

Received 11 June 2015; revised 17 July 2015; accepted 22 July 2015; posted 22 July 2015 (Doc. ID 242536); published 6 August 2015

We propose a method to optimally synthesize a strong 800-nm Ti:sapphire laser pulse and a relatively weak mid-infrared laser pulse to enhance harmonic yields in the water-window region. The required wavelength of the mid-infrared laser is varied from about 2.0 to 3.2 μm. The optimized waveforms generate comparable harmonic yields as the waveforms proposed in [Sci. Rep. 4, 7067 (2014)], but with much weaker intensity for the mid-infrared laser. This method provides an alternative scheme based on the available laser technology to help realize tabletop light source in the water-window region by high-order harmonic generation.

OCIS codes: (020.2649) Strong field laser physics; (190.4160) Multiharmonic generation; (320.7090) Ultrafast lasers; (340.7480) X-rays, soft x-rays, extreme ultraviolet (EUV).

http://dx.doi.org/10.1364/OL.40.003754

Powerful coherent x-ray light sources between the K-absorption edges of carbon (284 eV) and oxygen (543 eV), the so-called "water window," are highly attractive for high-contrast biological imaging because water is comparatively transparent, while nitrogen, carbon, and other elements contained in biological objects are absorbing. Furthermore, ultrafast water-window soft x-ray pulses can be used for the time-resolved study of biological molecules. Besides large-scale facilities such as synchrotron radiations and free-electron lasers, soft x-ray high-order harmonic generation (HHG) has been demonstrated in this region by using either traditional 800-nm Ti:sapphire lasers [1] or recently the mid-infrared (MIR) lasers [2–7]. However, the conversion efficiency of HHG is still too low for most applications in science and technology.

One of the possible ways to improve the harmonic efficiency from each atom is to modify the ionization and propagation of an electron in a laser field by using a tailored waveform. This can be achieved by synthesizing multi-color sinusoidal laser pulses to generate an arbitrary waveform for the optical driver [8–18]. Recently, we proposed a general scheme to significantly enhance the harmonic yield from a single atom, by synthesizing two- or three-color fields with optimized laser parameters [19]. We also showed how to extend the harmonic plateau to the water-window and the keV region by optimizing a waveform consisting of a strong MIR laser and a few percent of its third harmonic [20]. This approach requires a high-power MIR laser and a strong phase-controlled third harmonic. In reality, most wavelength-tunable, carrier-envelope-phase (CEP)-stabilized MIR lasers are pumped by 800-nm Ti:sapphire lasers, thus the pulse energies of the MIR are usually smaller than the pump lasers [6,7]. An alternative method is to synthesize an intense 800-nm Ti:sapphire laser with a relatively weak long-wavelength MIR to improve harmonic yield. Some results have shown that by combining the 800-nm laser with the MIR, continuum harmonic spectra are generated [9], the cutoff energy is extended, and the harmonic yield is enhanced [11]. The pulse synthesis also constructs a sub-cycle waveform [13], improves the one-color wavelength scaling [21], produces isolated attosecond pulses [12,16], and enhances the harmonic flux in the extreme ultraviolet (XUV) [18]. In spite of these efforts, waveform optimization has not been attempted, particularly for generating high harmonics in the water window.

In this Letter, we demonstrate that the synthesized waveform consisting of a strong 800-nm laser and a relatively weak MIR laser may be optimized such that harmonic cutoff energy is extended to the water window and the yield is greatly enhanced. In this optimization scheme, a high-power MIR laser is not needed. The resulting harmonic yields are slightly less than those using the previous method [20] where a weak third-harmonic pulse is used for synthesis. We will also investigate whether further enhancement of harmonic yield is possible by adding another color, i.e., in a three-color optimization.

The two-color waveform is written as

$$E(t) = A(t)[E_1 \cos(\omega_1 t + \phi_1) + E_2 \cos(\omega_2 t + \phi_2)]. \quad \textbf{(1)}$$

Here the two colors have the same temporal Gaussian envelope: $A(t) = \exp[-(2 \ln 2)t^2/\tau^2]$, τ is the full width at half maximum (FWHM) duration, E_i, ω_i, and ϕ_i $(i = 1, 2)$ are the respective amplitudes, angular frequencies, and CEPs of the two colors. In the optimization, λ_1 is fixed at 800 nm, $\phi_1 = 0$, and E_1 is larger than E_2. We search parameters $\{E_1, E_2, \omega_2, \phi_2\}$ to maximize single-atom HHG yield and to achieve the given cutoff energy. The detailed procedure of optimization is given in Ref. [20], employing strong-field approximation (SFA) [22], Newton's equation of electron motion, Ammosov–Delone–Krainov (ADK) formula, and standard genetic algorithm. The fitness function is the returning electron wave packet of the cutoff harmonic. The differences of this study from our previous works [19,20] are: (a) the short-wavelength (800-nm) laser is the major color. (b) The optimization is carried out over the whole laser pulse instead of a single optical cycle. (c) The resulting optimal wavelength of the MIR laser is not necessarily a multiple of the 800 nm, i.e., the two colors are incommensurate. (d) The constraints on the emission of "short"- and "long"-trajectory electrons are not imposed. The FWHM duration is 21.3 fs (8 optical cycles of the 800-nm laser), the ionization level over the whole pulse is 4%, and Ne is chosen as the target atom.

We summarize the optimized laser parameters in Table 1. The cutoff energy is varied from 200 to 550 eV, which covers the water-window region. From the optimized results, the peak intensity of the 800-nm laser is quite stable at $\sim 2.0 \times 10^{14}$ W/cm^2, while the intensity and wavelength of the MIR laser increases monotonically with the increase of the cutoff energy. The optimized phases are localized in three equivalent regions—around 1.5π, 0.9π, and 0.3π. In the meantime, for the cutoff energy above 350 eV, λ_2 is close to three times the wavelength of 800 nm. This wavelength ratio is similar to the $\omega + 3\omega$ optimization method we used previously [19,20], except that the shorter wavelength laser is the intense color in the present case. (Note that if $\lambda_2 = 2400$ nm, the change of 0.67π in ϕ_2 is equivalent to 2.0π for the 800-nm laser, thus explaining the three equivalent phase regions above.)

The waveforms for the two cutoff energies of 350 and 500 eV are shown in Fig. 1(a), together with the classical trajectories for electrons with maximum returning energies. At the two different cutoff energies, electrons are recombined at the same time where the vector potential is at the maximum, but they have different ionization times. In the 350-eV case, the electron has a smaller maximum displacement, shorter excursion time, and higher ionization electric field, leading to a stronger returning electron wave packet (REWP), as compared to the 500-eV case shown in Fig. 1(b). In Fig. 1(b), the decrease of the REWP from 200 to 500 eV is only about a factor of 5. The REWP is calculated by the SFA [22] in the spirit of the quantitative rescattering (QRS) model [23]. It is defined in the frequency domain as $W(\omega) = D(\omega)/d(\omega)$, where $D(\omega)$ is the Fourier transform of the laser induced dipole, and $d(\omega)$ is the photo-recombination transition dipole from the continuum state to the ground state. The isolated attosecond pulse would be more readily generated with synthesized waveform pulses if one spectrally filters out the cutoff harmonics.

We then check the stability of the optimized waveforms, and take the 350-eV waveform as an example, in which the optimal value of ϕ_2 is 0.24π. We vary ϕ_2 and show the single-atom HHG ($\propto \omega^4 |D(\omega)|^2$) spectra in Fig. 2. It clearly shows that harmonic yields and cutoff energies are stable only when ϕ_2 is varied by about 0.07π compared to the optimal value. This variation of 0.07π in ϕ_2 equals the time shift of about 250 as. Experimentally, the relative time drift between two colors could be controlled within about 250 as [13]

Table 1. Optimized Laser Parameters with Varied Cutoff Energies[a]

Cutoff Energy (eV)	$\lvert E_1\rvert^2$	$\lvert E_2\rvert^2$	λ_2	ϕ_2
200	2.06	1.00	1748	1.49π
300	2.03	1.11	1998	0.89π
350	2.06	1.19	2126	0.24π
400	2.07	1.34	2227	0.25π
450	2.02	1.58	2281	0.94π
500	2.00	1.76	2330	0.28π
550	2.02	1.90	2414	0.96π

[a]Laser intensities ($|E_1|^2$ and $|E_2|^2$) are in units of 10^{14} W/cm^2, and wavelength (λ_2) is given in nm. λ_1 is 800 nm.

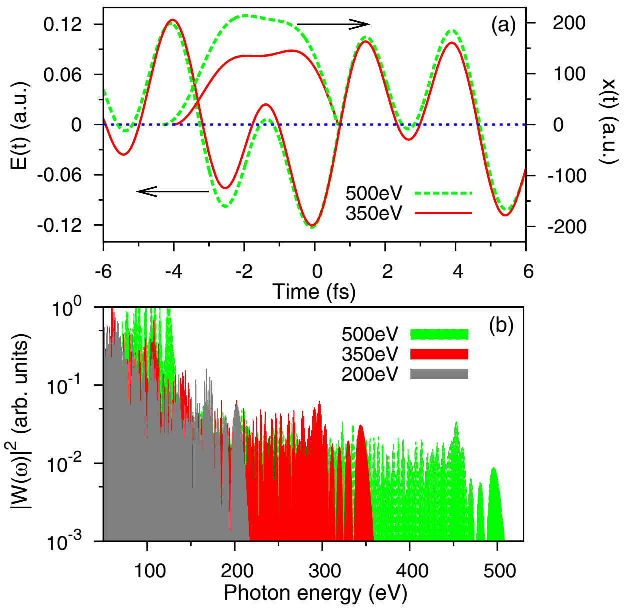

Fig. 1. (a) Optimized waveforms (in the central part) for two cutoff energies and the corresponding displacements $x(t)$ for the returning electrons. (b) Returning electron wave packets $W(\omega)$ with the varied cutoff energies as indicated.

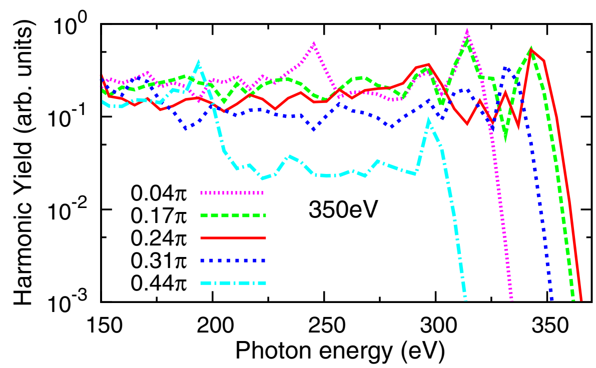

Fig. 2. Dependence of the single-atom HHG spectra on the relative phase ϕ_2. Only in a narrow region (from 0.17π to 0.31π), harmonic yields and cutoff energies are stable compared to the optimal one, i.e., 0.24π. The HHG spectra are calculated by using the QRS and smoothed by using the Bezier curve.

and 300 as [16]. Thus the optimized waveform is reachable with the current laser technology.

Since experimentally measured high harmonics are determined by both the emission from single atom and macroscopic propagation in the gas medium, we need to rely on complete simulation to predict observable harmonic yields. We simulate the propagated HHG spectra using the standard methods: the QRS model [23] is used to calculate the single-atom response, and three-dimensional Maxwell's equations are solved for both harmonics and the driver pulse [24]. Laser beam waist w_0 for each color is fixed at 50 μm, and the gas jet (1 mm long) is put at 2 mm after the focus. Gas pressure with uniform distribution in the jet is 10 Torr. The pulse duration is fixed at 21.3 fs for both colors. The optimized waveform is achieved only at the center of the gas jet. Four different simulations are shown in Fig. 3(a) for target cutoff energy near 350 eV, with nearly identical total pulse energy. Clearly, a single-color 800-nm laser cannot get to 350 eV. A 1925-nm laser reaches the required cutoff, but with the yield about 1000 times weaker than the 800-nm one. This is the consequence of the well-known unfavorable HHG wavelength scaling of single-color lasers [25]. With

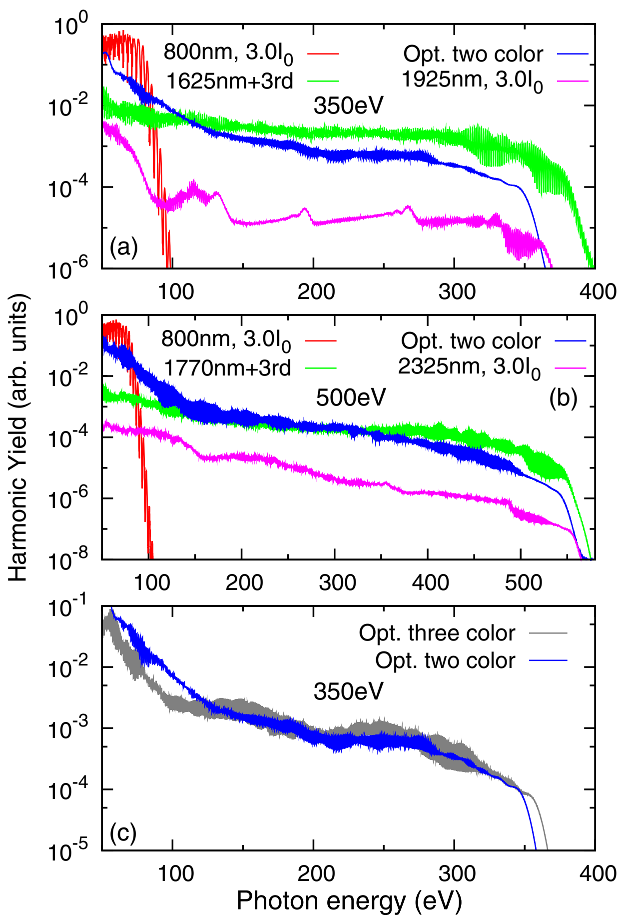

Fig. 3. Macroscopic HHG spectra with different cutoff energies calculated by using the QRS model. Comparison of the optimized two color (from Table 1) with two-color waveform (MIR laser and its 3rd harmonic) proposed in [20]: (a) 350 eV and (b) 500 eV. One-color results are shown for reference. The parameters are indicated in the figures, I_0 is in the units of 10^{14} W/cm^2. (c) Comparison of optimized two- and three-color (from Table 2) waveforms for the cutoff energy of 350 eV.

two-color optimized waveforms, the HHG yields over the same spectral range can be increased by about 30 to 100 times with the comparable total laser energy. The one with 1625 nm (3.88×10^{14} W/cm^2) plus its third harmonic (shown in Table 2 in [20] with a slightly larger cutoff energy) gives the highest yield. This method requires more than 10% of the 3rd harmonic energy that is challenging to achieve in the laboratory at present. With the current scheme, by combining 800-nm and 2126-nm laser pulses, where the latter has about 50% of the energy of the former, the generated harmonics over the same spectral region are only a factor of two or four smaller, while the total power is slightly smaller. Note that 2126-nm laser can be obtained by optical parametric amplification (OPA) or optical parametric chirped-pulse amplification (OPCPA) methods [5]. Such two-color experiments have been reported in a number of experiments [9,11–13,16,18], but the wavelength and relative powers between the two colors have not been optimized. Similar comparisons are shown in Fig. 3(b) for the cutoff energy of 500 eV, and the similar conclusion can be drawn. Comparing to harmonic yields by 800 nm in the XUV region (cutoff less than 100 eV), with two-color optimized fields, the HHG yield is about 10^3 times weaker for cutoff at 350 eV and 10^4 at 500 eV. In each case, the two-color pulses are about 10 to 100 times stronger than the single-color ones. The above comparison is made for the same gas pressure. For long-wavelength lasers, harmonic yields can be enhanced by further increasing the gas pressure [26]. Global optimization of the macroscopic conditions has been carried out recently in [27].

Can the harmonic yield be increased further by adding another color? With all the other conditions staying more or less the same, we add a 400-nm laser as the third color, and optimize its peak intensity $|E_3|^2$ and CEP ϕ_3 together with $\{E_1, E_2, \omega_2, \phi_2\}$. The parameters after the optimization are shown in Table 2 for the cutoff energy of 350 eV. The harmonic spectrum by the three-color waveform is shown in Fig. 3(c) in comparison with the two-color one. The two waveforms generate about the same harmonic yields, thus adding one more color does not help further enhancement of the harmonic yield.

In Table 1, the intensity of the MIR laser is only slightly smaller than the 800-nm laser. Can we decrease the relative intensity of the MIR laser? It can be done by increasing its

Table 2. Optimized Laser Parameters for the Three-Color Waveform[a]

$\|E_1\|^2$	$\|E_2\|^2$	$\|E_3\|^2$	λ_2	ϕ_2	ϕ_3
2.03	0.97	0.12	2356	1.55π	1.30π

[a]The cutoff energy is at 350 eV. The wavelength (λ_3) of the third color is set as 400 nm. Laser peak intensities ($|E_1|^2$, $|E_2|^2$, and $|E_3|^2$) are in units of 10^{14} W/cm^2, and laser wavelength (λ_2) is given in nm.

Table 3. Same as Table 1, but the Wavelength (λ_2) of the Mid-Infrared Laser is Preset

Cutoff Energy (eV)	$\|E_1\|^2$	$\|E_2\|^2$	λ_2	ϕ_2
350	2.15	0.97	2400	0.83π
350	2.17	0.87	2800	0.05π
500	2.02	1.28	2800	0.36π
500	2.12	1.00	3200	0.58π

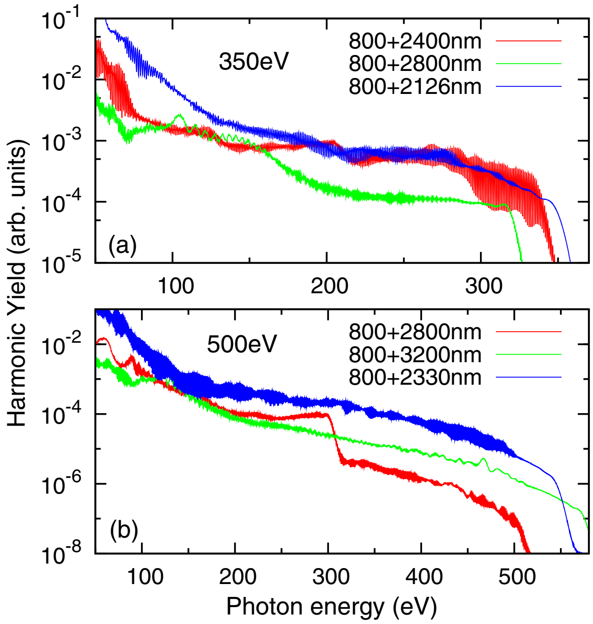

Fig. 4. Comparison of macroscopic HHG spectra by using optimized two-color waveforms in Table 1 and the waveforms shown in Table 3. Shown are for two cutoff energies: (a) 350 eV and (b) 500 eV.

wavelength. For the selected cutoff energy of 350 eV, we set the MIR laser at the longer wavelength of 2400 and 2800 nm, respectively. The resulting optimized parameters $\{E_1, E_2, \phi_2\}$ are shown in Table 3. The phase of 0.83π in the 2400-nm laser is equivalent to 1.51π in the 800-nm laser, which agrees with our previous works [19,20]. The combination of $(800 + 2400)$ nm is able to generate almost the same spectrum as the $(800 + 2126)$-nm combination. The corresponding macroscopic HHG spectra are shown in Fig. 4(a) in comparison with the wavelength optimized ones in Fig. 3. For the cutoff energy of 500 eV, we set the MIR at 2800 and 3200 nm, respectively. Using 3200 nm makes the harmonic yields weaker than by using 2330 nm, but still quite close to the optimized one; see Fig. 4(b). These combinations can also be considered as good solutions for generating high harmonics in the water window. This result shows that the optimal parameters are rather flexible in real experimentations.

In summary, we suggested a new scheme of optimizing the waveform for generating high harmonics in the water-window region, which is different from our previous proposal in [20]. The 800-nm Ti:sapphire laser pulse is chosen as a strong color, and the relatively weak MIR laser pulse is optimized in terms of its wavelength, intensity, and phase. Combining the enhancement of HHG yield using synthesized waves, shown in this study, with the emerging hundreds kHz or MHz high-repetition-rate laser technologies [28], the potential for generating high-flux high-harmonic soft x-rays in the water-window region as a powerful tabletop light source is very promising.

Funding. Air Force Office of Scientific Research (AFOSR) (FA9550-14-1-0255); U.S. Department of Energy (DOE).

REFERENCES

1. C. Spielmann, N. H. Burnett, S. Sartania, R. Koppitsch, M. Schnürer, C. Kan, M. Lenzner, P. Wobrauschek, and F. Krausz, Science **278**, 661 (1997).
2. E. J. Takahashi, T. Kanai, K. L. Ishikawa, Y. Nabekawa, and K. Midorikawa, Phys. Rev. Lett. **101**, 253901 (2008).
3. H. Xiong, H. Xu, Y. Fu, J. Yao, B. Zeng, W. Chu, Y. Cheng, Z. Xu, E. J. Takahashi, K. Midorikawa, X. Liu, and J. Chen, Opt. Lett. **34**, 1747 (2009).
4. M.-C. Chen, P. Arpin, T. Popmintchev, M. Gerrity, B. Zhang, M. Seaberg, D. Popmintchev, M. M. Murnane, and H. C. Kapteyn, Phys. Rev. Lett. **105**, 173901 (2010).
5. K.-H. Hong, C.-J. Lai, J. P. Siqueira, P. Krogen, J. Moses, C.-L. Chang, G. J. Stein, L. E. Zapata, and F. X. Kärtner, Opt. Lett. **39**, 3145 (2014).
6. N. Ishii, K. Kaneshima, K. Kitano, T. Kanai, S. Watanabe, and J. Itatani, Nat. Commun. **5**, 3331 (2014).
7. S. L. Cousin, F. Silva, S. Teichmann, M. Hemmer, B. Buades, and J. Biegert, Opt. Lett. **39**, 5383 (2014).
8. I. J. Kim, C. M. Kim, H. T. Kim, G. H. Lee, Y. S. Lee, J. Y. Park, D. J. Cho, and C. H. Nam, Phys. Rev. Lett. **94**, 243901 (2005).
9. C. Vozzi, F. Calegari, F. Frassetto, L. Poletto, G. Sansone, P. Villoresi, M. Nisoli, S. De Silvestri, and S. Stagira, Phys. Rev. A **79**, 033842 (2009).
10. H.-C. Bandulet, D. Comtois, E. Bisson, A. Fleischer, H. Pépin, J.-C. Kieffer, P. B. Corkum, and D. M. Villeneuve, Phys. Rev. A **81**, 013803 (2010).
11. T. Siegel, R. Torres, D. J. Hoffmann, L. Brugnera, I. Procino, A. Zaïr, J. G. Underwood, E. Springate, I. C. E. Turcu, L. E. Chipperfield, and J. P. Marangos, Opt. Express **18**, 6853 (2010).
12. E. J. Takahashi, P. Lan, O. D. Mücke, Y. Nabekawa, and K. Midorikawa, Phys. Rev. Lett. **104**, 233901 (2010).
13. S.-W. Huang, G. Cirmi, J. Moses, K.-H. Hong, S. Bhardwaj, J. R. Birge, L.-J. Chen, E. Li, B. J. Eggleton, G. Cerullo, and F. X. Kärtner, Nat. Photonics **5**, 475 (2011).
14. A. Wirth, M. Th. Hassan, I. Grguraš, J. Gagnon, A. Moulet, T. T. Luu, S. Pabst, R. Santra, Z. A. Alahmed, A. M. Azzeer, V. S. Yakovlev, V. Pervak, F. Krausz, and E. Goulielmakis, Science **334**, 195 (2011).
15. P. Wei, J. Miao, Z. Zeng, C. Li, X. Ge, R. Li, and Z. Xu, Phys. Rev. Lett. **110**, 233903 (2013).
16. E. J. Takahashi, P. Lan, O. D. Mücke, Y. Nabekawa, and K. Midorikawa, Nat. Commun. **4**, 2691 (2013).
17. S. Haessler, T. Balčiunas, G. Fan, G. Andriukaitis, A. Pugžlys, A. Baltuška, T. Witting, R. Squibb, A. Zaïr, J. W. G. Tisch, J. P. Marangos, and L. E. Chipperfield, Phys. Rev. X **4**, 021028 (2014).
18. L. V. Dao, K. B. Dinh, and P. Hannaford, Nat. Commun. **6**, 7175 (2015).
19. C. Jin, G. Wang, H. Wei, A. T. Le, and C. D. Lin, Nat. Commun. **5**, 4003 (2014).
20. C. Jin, G. Wang, A. T. Le, and C. D. Lin, Sci. Rep. **4**, 7067 (2014).
21. P. Lan, E. J. Takahashi, and K. Midorikawa, Phys. Rev. A **81**, 061802 (2010).
22. M. Lewenstein, P. Balcou, M. Y. Ivanov, A. L'Huillier, and P. B. Corkum, Phys. Rev. A **49**, 2117 (1994).
23. A. T. Le, R. R. Lucchese, S. Tonzani, T. Morishita, and C. D. Lin, Phys. Rev. A **80**, 013401 (2009).
24. C. Jin, A. T. Le, and C. D. Lin, Phys. Rev. A **83**, 023411 (2011).
25. J. Tate, T. Auguste, H. G. Muller, P. Salières, P. Agostini, and L. F. DiMauro, Phys. Rev. Lett. **98**, 013901 (2007).
26. T. Popmintchev, M.-C. Chen, A. Bahabad, M. Gerrity, P. Sidorenko, O. Cohen, I. P. Christov, M. M. Murnane, and H. C. Kapteyn, Proc. Natl. Acad. Sci. USA **106**, 10516 (2009).
27. C. Jin, G. J. Stein, K.-H. Hong, and C. D. Lin, Phys. Rev. Lett. **115**, 043901 (2015).
28. M. Krebs, S. Hädrich, S. Demmler, J. Rothhardt, A. Zaïr, L. Chipperfield, J. Limpert, and A. Tünnermann, Nat. Photonics **7**, 555 (2013).